Analysis and development of fourth order LCLC resonant based capacitor charging power supply for pulse power applications

P. Naresh,[a] C. Hitesh, A. Patel,[b] T. Kolge, Archana Sharma, and K. C. Mittal
Homi Bhabha National Institute, Accelerator and Pulse Power Division, Bhabha Atomic Research Centre, Trombay, Mumbai 400 085, India

(Received 23 April 2013; accepted 5 August 2013; published online 22 August 2013)

A fourth order (LCLC) resonant converter based capacitor charging power supply (CCPS) is designed and developed for pulse power applications. Resonant converters are preferred t utilize soft switching techniques such as zero current switching (ZCS) and zero voltage switching (ZVS). An attempt has been made to overcome the disadvantages in 2nd and 3rd resonant converter topologies; hence a fourth order resonant topology is used in this paper for CCPS application. In this paper a novel fourth order LCLC based resonant converter has been explored and mathematical analysis carried out to calculate load independent constant current. This topology provides load independent constant current at switching frequency (f_s) equal to resonant frequency (f_r). By changing switching condition (on time and dead time) this topology has both soft switching techniques such as ZCS and ZVS for better switching action to improve the converter efficiency. This novel technique has special features such as low peak current through switches, DC blocking for transformer, utilizing transformer leakage inductance as resonant component. A prototype has been developed and tested successfully to charge a 100 μF capacitor to 200 V. © *2013 AIP Publishing LLC*. [http://dx.doi.org/10.1063/1.4818948]

I. INTRODUCTION

In recent years pulsed power technology is being used for industrial applications such as food processing, medical and water treatment, ion implantation, and welding. Accelerator and pulse power division use this technology for the generation of electron beam, high power microwave, and flash X-ray. More applications and recent work on pulse power technology were discussed in Ref. 1. Pulsed power systems have the primary energy storage systems in which energy storage capacitor is used to store energy for longer duration and discharges across the pulsed load for very short duration of time.

A suitable power supply is necessary to charge these pulsed power systems, so called capacitor charging power supply, in which constant current technique is more popularly used. Resonant based converters are extensively used to minimize the switching losses and to get constant current, since the load is capacitor it needs to be charged with constant current from the beginning.

Second order series LC resonant based capacitor charging power supply is extensively used for pulsed power applications operated in discontinuous conduction mode, its current characteristics discussed in Ref. 2 explained how the peak current increases through switches.

Parallel resonant topology is another topology which can works as constant current source when switching frequency is equal to the resonant frequency and it was explored in Ref. 3, where the author discussed the variation in the current gain with respect to normalized frequency for particular Q value.

LCL resonant converter is another attractive topology that can be used as inherent constant current source when its resonant frequency is exactly equal to switching frequency. With the usage of clamp diodes it can provide CC-CV at the output as was explored previously in Ref. 4. Design and development of LCL resonant based topology have been utilized for repetitive operation for capacitor charging power supply application in Ref. 5 in which zero current switching was utilized. Second, third, and fourth order resonant converter topologies were explored in Ref. 6 and analyzed as immittance converter for different applications, where the author explained which particular topology can be used as constant current topology.

All the topologies which were discussed previously are having considerable advantages and disadvantages. In view of these, we propose a fourth order (LCLC) resonant based topology which can be utilized to design a capacitor charging power supply.

The proposed topology will provide load independent constant current, inherent short circuit proof, which utilizes soft switching techniques like zero current switching (ZCS) and zero voltage switching (ZVS) for low loss in the inverter circuit. The main advantage with fourth order is that it limits the peak currents flowing through semiconductor switches as compared to the series and parallel resonant converters, which minimizes the paralleling of switches and eliminate complex cooling system for the inverter circuit. The basic building blocks are shown in block diagram in Fig. 1.

In this paper a detailed analysis is done to ensure load independent constant current and zero current switching. Proposed fourth order LCLC topology mathematical analysis and operation have been discussed in Secs. II and III. In Sec. II, topology selection and mathematical analysis are discussed. Section III describes design and development features and operation which is followed by results and discussions in Sec. IV.

[a]Electronic mail: nareshp@barc.gov.in
[b]Electronic mail: aspatel@barc.gov.in

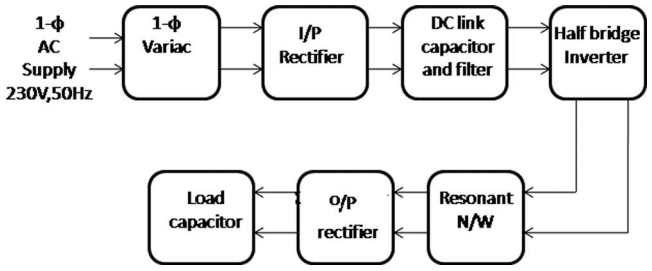

FIG. 1. Basic block diagram of CCPS.

II. FEATURES OF LCLC TOPOLOGY OVER LOWER ORDER TOPOLOGY AND MATHEMATICAL ANALYSIS OF LCLC RESONANT TOPOLOGY

A. Features of LCLC topology over lower order topology

Topology selection plays an important role in designing power supply for pulsed power applications, wherein energy storage capacitor acts as load. So, the topology should have inherent short circuit proof. Series LC, parallel LC, LCL, and CLC resonant based topologies have been proposed previously to design capacitor charging power supply for pulse power applications, but all these have some limitations.

Series LC resonant based converter has been used extensively for capacitor charging power supply, since it is having inherent short circuit property and provides constant current in discontinuous conduction mode. But the major disadvantage is that the peak current flowing through the inverter switches is very high. For higher charging rates parallel operation of switches is used to overcome peak current through the switches which increases size of the cooling system and power supply. Because of these limitations, the series resonant topology is not an attractive topology for high power applications.

Parallel LC resonant topology is another topology which can be used as constant current source when operated at switching frequency equal to resonant frequency. This topology also provides short circuit protection as well as it limits the peak current flowing through the switches. The peak current is lower as compared to series LC, but the main disadvantage is circulating currents which increases conduction losses per device, this, in turn, decreases the converter efficiency.

There are different combinations in third order topologies, but all third order topologies are not useful for constant current applications, except LCL and CLC, which can be used as constant current source operated at resonant frequency equal to switching frequency. This topology has the advantages that the current through the switches is much lesser compared to series LC, parallel LC, and CLC resonant converter topology, in addition we can use transformer leakage inductance as resonant inductor. On the other hand, the LCL-T RC does not inherently provide DC blocking for the isolated high frequency transformer and an additional bulky DC blocking capacitor may be required in practice.

Further, the transformer winding capacitance, which can be significant in high-voltage transformer, is not gainfully utilized as resonant component can significantly affect the converter characteristics. A CLC resonant converter can also be used as constant current source like LCL and it can block the DC when used with high frequency transformer, but the main drawback is circulating currents which can lead the additional losses in inverter circuit like in parallel resonant converter.

In this paper, the focus was to overcome the limitations of series LC, parallel LC, LCL, and CLC resonant topologies. As the power rating increases (i.e., if the charging rate is in multiples of 10 kJ/s) the current through Insulated gate bipolar transistor (IGBT) also increases, there it needs the paralleling operation if it uses conventional series resonant and parallel resonant topology. In addition to this, the peak current flowing through the IGBTs is also very high. Instead of increasing IGBTs in inverter circuit by increasing the resonant components, we can overcome paralleling operation and complex cooling system by using the proposed topology. Here we proposed a new topology, so called fourth order resonant based converter topology for capacitor charging power supply applications. In this paper we carried out the mathematical analysis to find the load independent constant current and condition for zero current switching.

B. Mathematical analysis of LCLC resonant topology

In the proposed scheme L_1, C_1, L_2, and C_2 are connected in T structure as shown in Fig. 2(a). Inductor (L_1) and capacitor (C_1) are connected in series comprises reactance X_1, inductor (L_2) comprises reactance X_2 and capacitor (C_2) in branch three comprises reactance X_3. Mathematical analysis started with the equivalent circuit diagram is shown in Fig. 2(b).

$X_1 = X_3 = -X_2$ is the condition for resonant immittance converter

$$X_1 = X_1 = \frac{1-\omega^2 L_1 C_1}{j\omega C_1}, \quad X_2 = \mathrm{j}\omega L_2, \quad X_3 = \frac{1}{j\omega C_2},$$

where $\mathrm{x} = \frac{L_2}{L_1}$, $\mathrm{y} = \frac{C_2}{C_1}$, and $\mathrm{z} = \frac{8R_L}{n^2\pi^2}$.

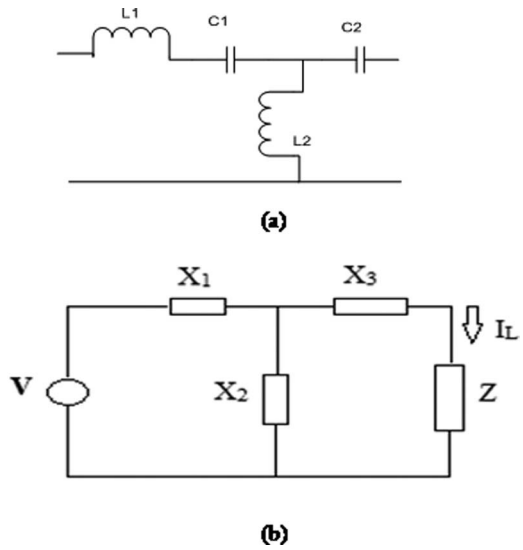

FIG. 2. Resonant converter. (a) T-structure. (b). T-structure for mathematical analysis.

On applying Kirchoffs voltage law (KVL) the voltage across X_2 is expressed by (1)

$$V_{X_2} = \frac{X_2 (Z + X_3) V}{X_1X_2 + X_1X_3 + X_2X_3 + Z (X_1 + X_2)}. \quad (1)$$

Then the current through load is expressed by

$$I_{Load} = \frac{V_{X_2}}{Z + X_3}, \quad (2)$$

$$I_{Load} = \frac{X_2 V}{X_1X_2 + X_1X_3 + X_2X_3 + Z (X_1 + X_2)}. \quad (3)$$

Solving Eq. (3) after substituting the values X_1, X_2, and X_3 makes the coefficient of z equal to zero, then the load current I_L becomes independent of z at $\omega_0 = \frac{1}{\sqrt{(1+x)L_1C_1}}$. Value of I_{Load} at ω_0 is $\frac{V}{\omega_0 L_1}$.

Circuit offers ZCS at resonance that can be obtained by making imaginary part of Z_{TOT} zero:

$$Z_{TOT} = \frac{X_1X_2 + X_1X_3 + X_2X_3 + Z (X_1 + X_2)}{X_2 + X_3 + Z}. \quad (4)$$

Solving Eq. (4) after substituting the values X_1, X_2, and X_3 we can obtain ZCS by making imaginary part of Z_{TOT} zero at ω_0 for 1 + x = xy. At this condition the source sees resistive nature of load, so the current and voltage of source are in the same phase. When the current becomes zero with respect to source voltage the switching action takes place in inverter circuit.

For the purpose of analysis, output rectifier and filter are replaced by an equivalent ac resistance and the fundamental sinusoidal equivalent is used instead of square wave input voltage source. The fundamental expressions have been given as

$$z = \frac{8R_L}{n^2\pi^2} \quad \text{and} \quad V = \frac{V_d 2\sqrt{2}}{\pi}.$$

The resonant frequency and normalized switching frequency are given as

$$\text{at y} = \frac{1+x}{x}, \quad \omega_0 = \frac{1}{\sqrt{(1+x)L_1C_1}} \quad \text{and} \quad \omega_n = \frac{\omega}{\omega_0}.$$

Characteristic impedance of the resonant circuit and Q are given as

$$Z_n = \sqrt{\frac{L_1}{C_1}} \quad \text{and} \quad Q = \frac{n^2\omega_0 L_1}{R_L}.$$

Current gain, $H = \frac{nI_0}{V_d/Z_n}$ and voltage gain, $M = \frac{V_0/n}{V_d}$ are given as

$$H = \frac{xy\omega_n^3(\sqrt{1+x})}{-\frac{1}{Q}\omega_n y (1+x)\left(1-\omega_n^2\right) + j\frac{\pi^2}{8}\left[\left(1-\omega_n^2\right)(1+x)^2 - \omega_n^2 xy\left(1+x-\omega_n^2\right)\right]}, \quad (5)$$

$$M = \frac{\omega_n^3 xy}{-\omega_n y (1+x)\left(1-\omega_n^2\right) + jQ\frac{\pi^2}{8}\left\{(1+x)^2\left(1-\omega_n^2\right) - \omega_n^2 xy\left(1+x-\omega_n^2\right)\right\}}. \quad (6)$$

Normalized current through and voltage across inductor L_1 (I_{L_1}, V_{L_1}), L_2 (I_{L_2}, V_{L_2}), C_1 (I_{c_1}, V_{c_1}), and C_2 (I_{c_2}, V_{c_2}) are derived with base voltage V_d and V_d/Z_n are as follows:

$$I_{L_{1,N}} = I_{c_1,N} = \frac{I_{L_1}, \text{rms}}{V_d/Z_n} = \frac{I_{c_1}, \text{rms}}{V_d/Z_n},$$

$$I_{L_{1,N}} = I_{c_1,N} = \frac{\pi\sqrt{1+x}\left\{\omega_n Q\left(1+x-\omega_n^2\right) + j\frac{y8\omega_n^2}{\pi^2}\right\}}{2\sqrt{2}\left[y\omega_n(1+x)\left(1-\omega_n^2\right) + j\frac{\pi^2 Q\left\{xy\omega_n^2\left(1+x-\omega_n^2\right)-(1+x)^2\left(1-\omega_n^2\right)\right\}}{8}\right]}, \quad (7)$$

$$I_{L_2,N} = \frac{I_{L_2}, rms}{V_d/Z_n} = \frac{\pi\sqrt{1+x}\left\{\omega_n Q(1+x) + j\frac{y8\omega_n^2}{\pi^2}\right\}}{2\sqrt{2}\left[y\omega_n(1+x)\left(1-\omega_n^2\right) + j\frac{\pi^2 Q\left\{xy\left(1+x-\omega_n^2\right)-(1+x)^2\left(1-\omega_n^2\right)\right\}}{8}\right]}, \quad (8)$$

$$I_{C_2,N} = \frac{I_{C_2}, rms}{V_d/Z_n} = \frac{\pi xy\omega_n^3(\sqrt{1+x})}{2\sqrt{2}\left[-\frac{1}{Q}\omega_n y(1+x)\left(1-\omega_n^2\right) + j\frac{\pi^2}{8}\left\{\left(1-\omega_n^2\right)(1+x)^2 - \omega_n^2 xy(1+x+\omega_n^2)\right\}\right]}, \quad (9)$$

$$V_{L_{1,N}} = \frac{V_{L_{1,rms}}}{V_d} = \frac{-\pi\left\{\omega_n^2 Q\left(1+x-xy\omega_n^2\right) + j\frac{8\omega_n^3 y}{\pi^2}\right\}}{2\sqrt{2}\left[\frac{\pi^2}{8}Q\left\{(1+x)^2\left(1-\omega_n^2\right) - xy\omega_n^2\left(1+x-\omega_n^2\right)\right\} + j\omega_n y\left(1-\omega_n^2\right)(1+x)\right]}, \quad (10)$$

$$V_{L_{2,N}} = \frac{V_{L_{2,rms}}}{V_d} = \frac{-\pi\omega_n^2 x\left\{(1+x)\,Q + j\frac{8y\omega_n}{\pi^2}\right\}}{2\sqrt{2}\left[\frac{\pi^2}{8}\left\{(1+x)^2\left(1-\omega_n^2\right) - xy\omega_n^2\left(1+x-\omega_n^2\right)\right\} + jy\omega_n(1+x)\left(1-\omega_n^2\right)\right]}, \tag{11}$$

$$V_{C_{1,N}} = \frac{V_{C_{1,rms}}}{V_d} = \frac{\pi(1+x)\left[Q\left(1+x-xy\omega_n^2\right) + j\frac{8y\omega_n}{\pi^2}\right]}{2\sqrt{2}\left[\frac{Q\pi^2}{8}\left\{\left(1-\omega_n^2\right)(1+x)^2 - xy\omega_n^2\left(1-\omega_n^2\right)\right\} + j\omega_n y(1+x)\right]}, \tag{12}$$

$$V_{C_{2,N}} = \frac{V_{C_{2,rms}}}{V_d} = \frac{-\pi x(1+x)\omega_n^2}{2\sqrt{2}\left[\frac{\pi^2}{8}\left\{\left(1-\omega_n^2\right)(1+x)^2 - xy\omega_n^2\left(1+x-\omega_n^2\right)\right\} + j\frac{y(1+x)\omega_n}{Q}\right]}. \tag{13}$$

This topology can provide load independent constant current when $\omega_n = 1$, as shown in Fig. 3, where ω_n is the normalized frequency and is the ratio of ω_s to ω_o. In the mathematical analysis it was already showed that current is load independent (i.e., independent of Q), and is proved from the simulation also in Fig. 3. When $\omega_n = 1$ then the current gain (H) will become constant at any Q value. Other than $\omega_n = 1$ the current gain varies with respect to Q.

III. DEVELOPMENT FEATURES AND OPERATION OF LCLC RESONANT CONVERTER

A. Development features

The design parameters are calculated based on the equations derived in Sec. II and are as follows:

Input voltage = v_{dc} = 75 V.
Switching frequency = f_s = 25 kHz.
Charging voltage = V_{load} = 200 V.
J/s rating = 20 J/s.

$$\omega_0 = \frac{1}{(\sqrt{1+x})(\sqrt{L_1C_1})}, \quad f = \frac{1}{2\pi(\sqrt{1+x})(\sqrt{L_1C_1})}.$$

$$\omega_0 = \frac{1}{(\sqrt{1+x})(\sqrt{L_{r1}C_{r1}})}, \quad f = \frac{1}{2\pi(\sqrt{1+x})(\sqrt{L_{r1}C_{r1}})},$$

where $L_1 = L_{r1}$ and $C_1 = C_{r1}$.

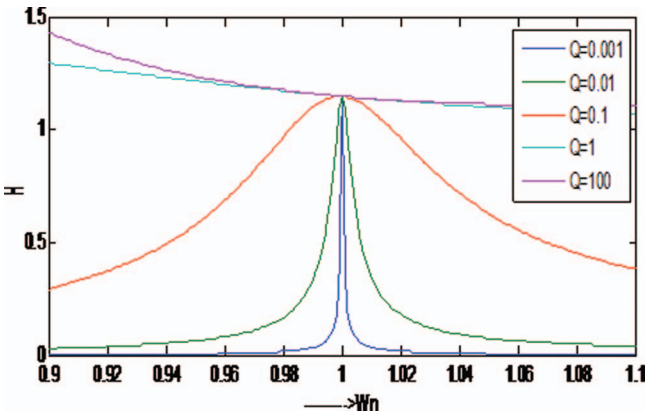

FIG. 3. Characteristics of current gain (H) vs normalized frequency (ω_n) for different Q values.

For f = 25 kHz

$$\omega_0 = 1.57 \times 10^5,\ \omega_0^2 = 2.467 \times 10^{10}$$

$$\omega_0^2 = \frac{1}{(1+x)(L_{r1}C_{r1})},$$

where x = 1, $2\omega_0^2 = \frac{1}{(L_{r1}C_{r1})}$, and $L_{r1}C_{r1} = 2.02 \times 10^{-11}$.

If C_{r1} = 23.5 nF (because it is available in laboratory)

$$L_{r1} = 862\,\mu H,\ L_{r2} = x \times L_{r1},$$

where x = 1 and L_{r2} = 862 μH.

$$y = \frac{1+x}{x} = 2,\ C_{r1} = 23.5\,nF,\ C_{r2} = 2 \times C_{r1},\ C_{r2} = 47\,nF,$$

$$V_{rms} = \frac{2\sqrt{2}V_d}{\pi}, \quad V_d = 75V, \quad V_{rms} = 67.54V,$$

$$I_{Load\,avg} = C_{load}\frac{dV}{dt},\ t_c = \text{charging time} = 100\,ms,$$

$$V = \frac{I_{avg} * t}{Cload}.$$

For charging the capacitor up to 200 V the current required,

$$I_{Load\,avg} = 0.2\,A = 200\,mA.$$

Peak current through the switches M_1 and M_2 is calculated at the end of the charging period, because current flowing through the switches depends on source voltage as well as voltage across the resonant capacitor (C_{r1}). The voltage increases in the resonant capacitor (C_{r1}) with progress in time as shown in Fig. 4. The source voltage and voltage across resonant capacitor (C_{r1}) come into the picture in each cycle, so the current flowing through the switches is the cumulative effect of source voltage and voltage across resonant capacitor (C_{r1}).

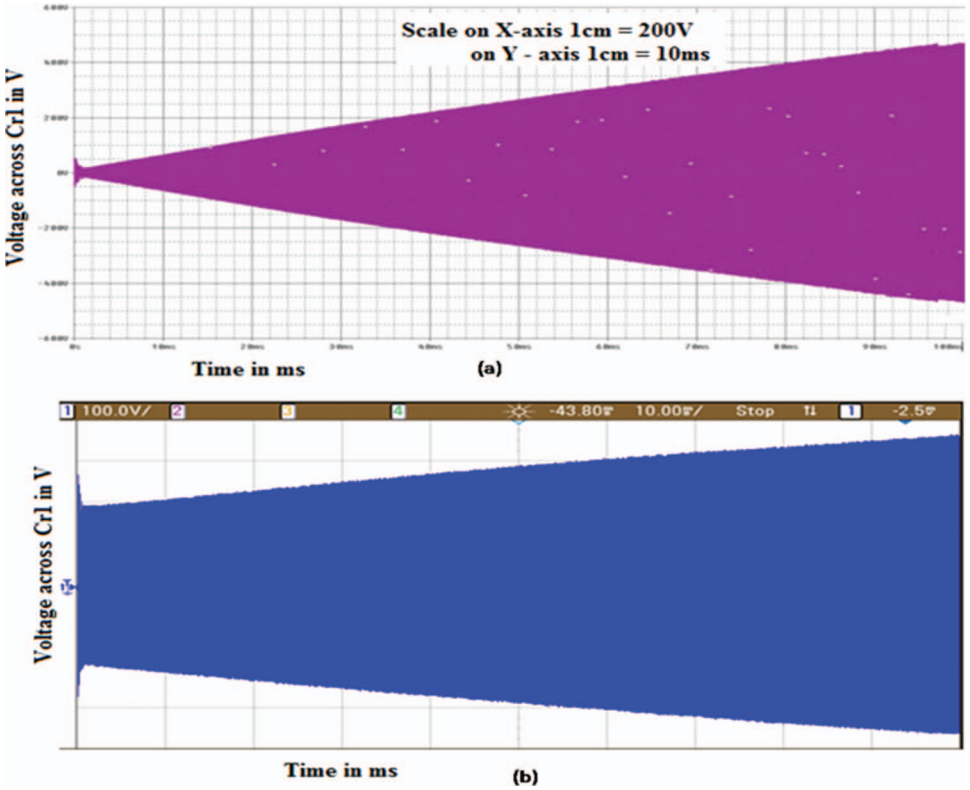

FIG. 4. Current through resonant capacitor C_{r1}. (a) Simulated; (b) experimental.

The current flowing through switches = current flowing through the resonant inductor (L_{r1}) and is given by

$$I_{L_{r_1}\,\text{peak}} = \frac{\text{peak input voltage} + \text{peak voltage across } C_{r1}}{Zn},$$

$$I_{L_{r1}}\,\text{peak} = \frac{V_{s\,peak} + VC_{r1\,peak}}{Zn},$$

where peak input voltage, $V_{s\,peak} = 47$ V, and $V_d = 37.5$ V.

Peak voltage across $C_{r1} = V_{C_{r1}\,peak} = 460$ V and $Z_n = 195\ \Omega$.

$$I_{Lr1peak} = \frac{47 + 460}{195} \approx 2.6 \text{ A}.$$

The following component values are used for simulation:

Resonant inductors = $L_{r1} = L_{r2} = 862\ \mu$H.
Resonant capacitor = $C_{r1} = 23.5$ nF.
Resonant capacitor = $C_{r2} = 47$ nF.
Input voltage = $v_{dc} = 75$ V.
Switching frequency = f_s = resonant frequency = $f_r = 25$ kHz.
Charging voltage = $V_{load} = 200$ V.

DC link capacitors = $C_1 = C_2 = 2.2$ mF (DC link capacitor is much higher than the first resonant capacitor, i.e., it should not alter the operation of resonant network). The schematic circuit diagram is shown in the Fig. 5. The experimental set up has shown in Fig. 13. We have developed own gate drivers and gate power supply in the lab to run inverter switches. Switching devices, MOSFETs (IRF840), are chosen, because the prototype was designed to carry 6 A peak current. MOSFET (IRF840) can carry continuous drain current of 8 A, the peak current flowing through each device is about 2.6 A at the end of charging. Output rectifier developed using high frequency fast diodes (BYM 26E) and discharge resistor bunch has been used for discharging the load capacitor manually. The component ratings are not exactly equal to the design parameters.

B. Operation

In the circuit operation first the DC link capacitors are charged to the 37.5 V each, in the first half of resonant cycle DC link capacitor (C_1), resonant network, MOSFET (M_1), diode (D_3), C_{load} (100 μF), and diode (D_6) comes into

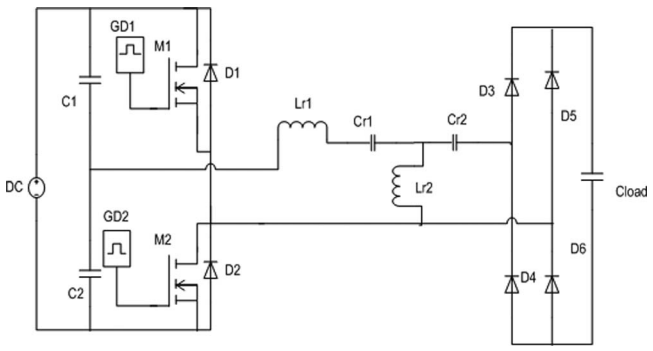

FIG. 5. Schematic circuit diagram of CCPS.

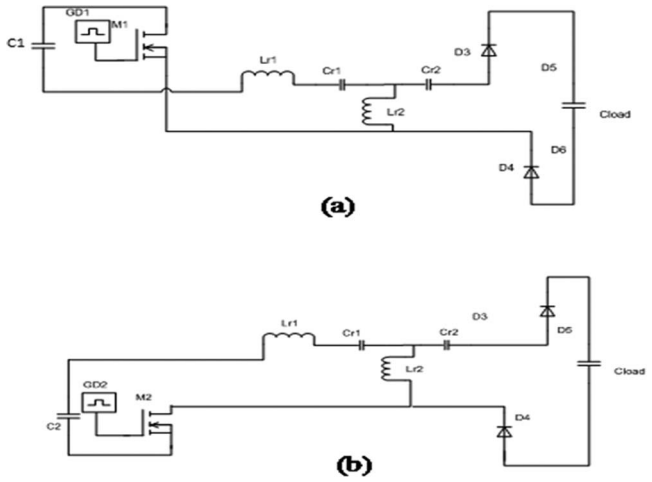

FIG. 6. Circuit diagram when MOSFET on. (a) M_1 on; (b) M_2 on.

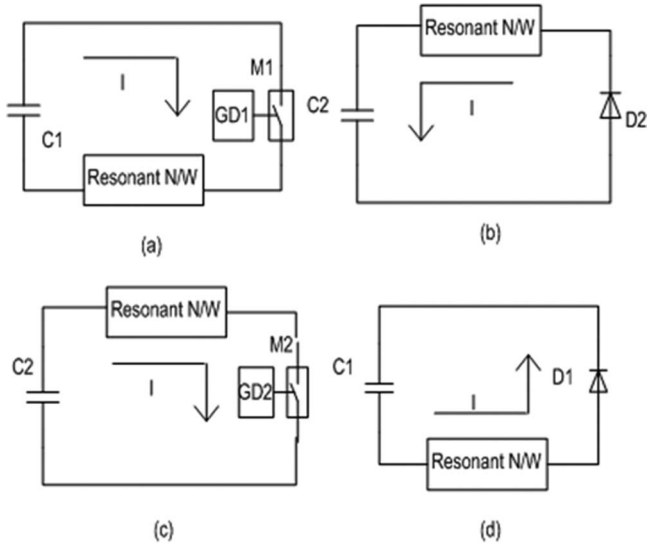

FIG. 8. Circuit diagrams of ZVS (a) in time t_1; (b) in time t_2; (c) in time t_3; and (d) in time t_4.

the picture as shown in Fig. 6(a). In the second half of resonant cycle DC link capacitor (C_2), resonant network, MOSFET (M_2), diode (D_4), C_{load} (100 μF), and diode (D_5) come into the picture as shown in Fig. 6(b). In both the half cycles the current flowing through the load is not going to change, nothing but the load capacitor charges linearly. The soft switching techniques zero current and zero voltage are main concern in the operation as explained in the next two paragraphs.

1. Zero current switching

Zero current switching is nothing but inverter switches turn off action takes place when current through the switch is zero. The current becomes zero in the circuit when switching frequency is equal to resonant frequency. At this condition the circuit becomes resistive in nature, so the inverter output voltage and current through the resonant inductor (Lr1) are in same phase. In the design, switching frequency chosen as 25 kHz and its time period becomes 40 μs, so the current becomes zero after every 20 μs. For every 20 μs switches will get turn on and turn off its equivalent circuit as shown in Figs. 6(a) and 6(b). The simulation and experimental results are shown in Fig. 10.

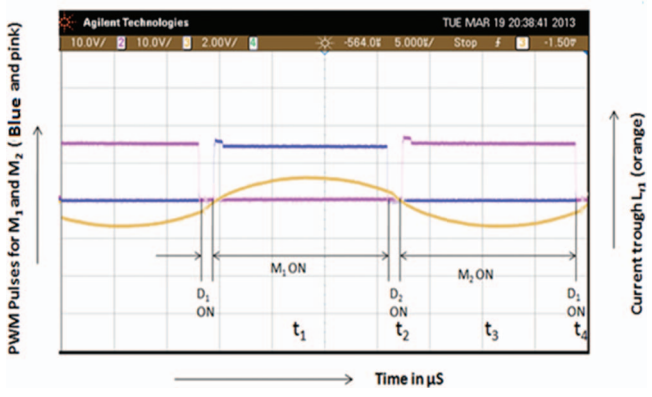

FIG. 7. Current wave form to explain ZVS.

2. Zero voltage switching

Zero voltage switching obtained by making the current to flow through the anti-parallel diodes of MOSFET switches M_1 and M_2, the operation explained on the basis of current wave form is shown in Fig. 7. During time t_1 MOSFET M_1 is switched on and the current direction through the load is shown in Fig. 8(a). When the switch M_1 is turned off current still remains in the same direction but the circuit completes through C_2, diode (D_2), and resonant network (shown in Fig. 8(b)) by adjusting the dead time between M_1 and M_2. During the time t_3 when MOSFET M_2 is switched on, the current direction through the resonant network is reversed as shown in Fig. 8(c), during the time t_4 diode (D_1) of MOSFET (M_1) gets forward biased, after turning off the switch M_2 the current through the resonant network still remains in same direction and circuit completes through load, C_1, resonant network, and diode (D_1) as shown in Fig. 8(d) in the dead time period.

IV. RESULTS

Simulation and experimental results are obtained for the circuit shown in Fig. 5. Component values are obtained from the mathematical analysis.

A. Simulation results

Simulation results are obtained from ORCAD spice simulation tool for the 100 μF load capacitor. Fig. 9(a) describes how current linearly increases with time, this rms current will flow through the first resonant inductor L_{r1}. The magnified wave form of this resonant current is shown in Fig. 10(a). The voltage profile across resonant capacitor (C_{r1}), which is useful in finding the peak current flowing through the switches M_1 and M_2 is already shown in Fig. 4(a). The voltage profile across the load capacitor (V_{load}) vs. time is sown in

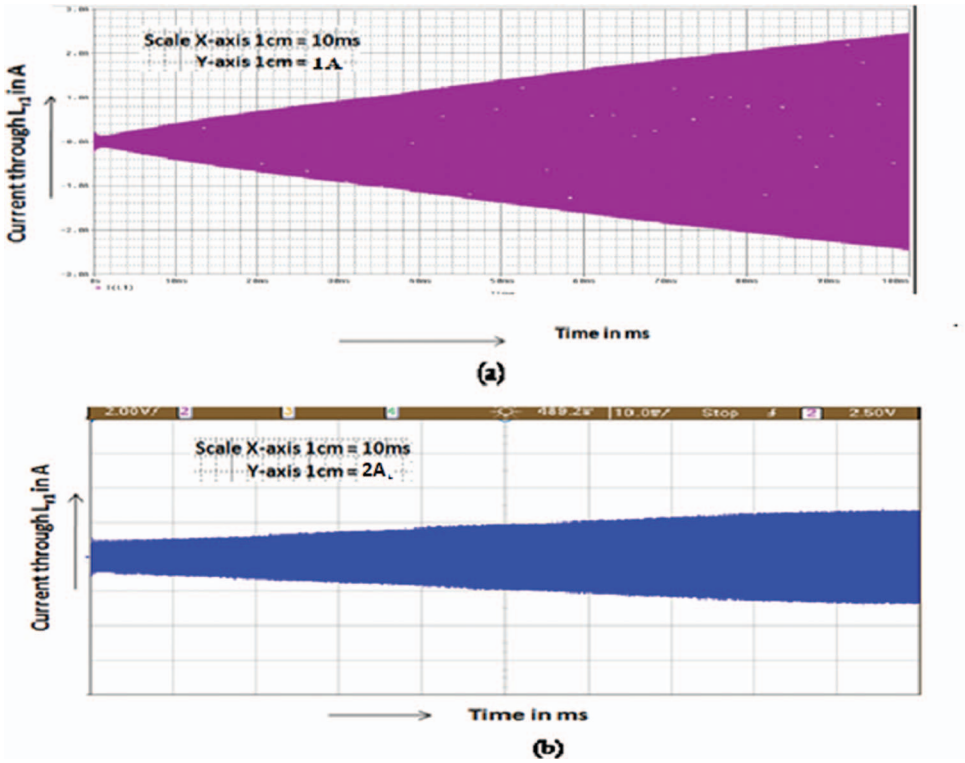

FIG. 9. Current through resonant inductor L_{11}: (a) Simulated; (b) experimental.

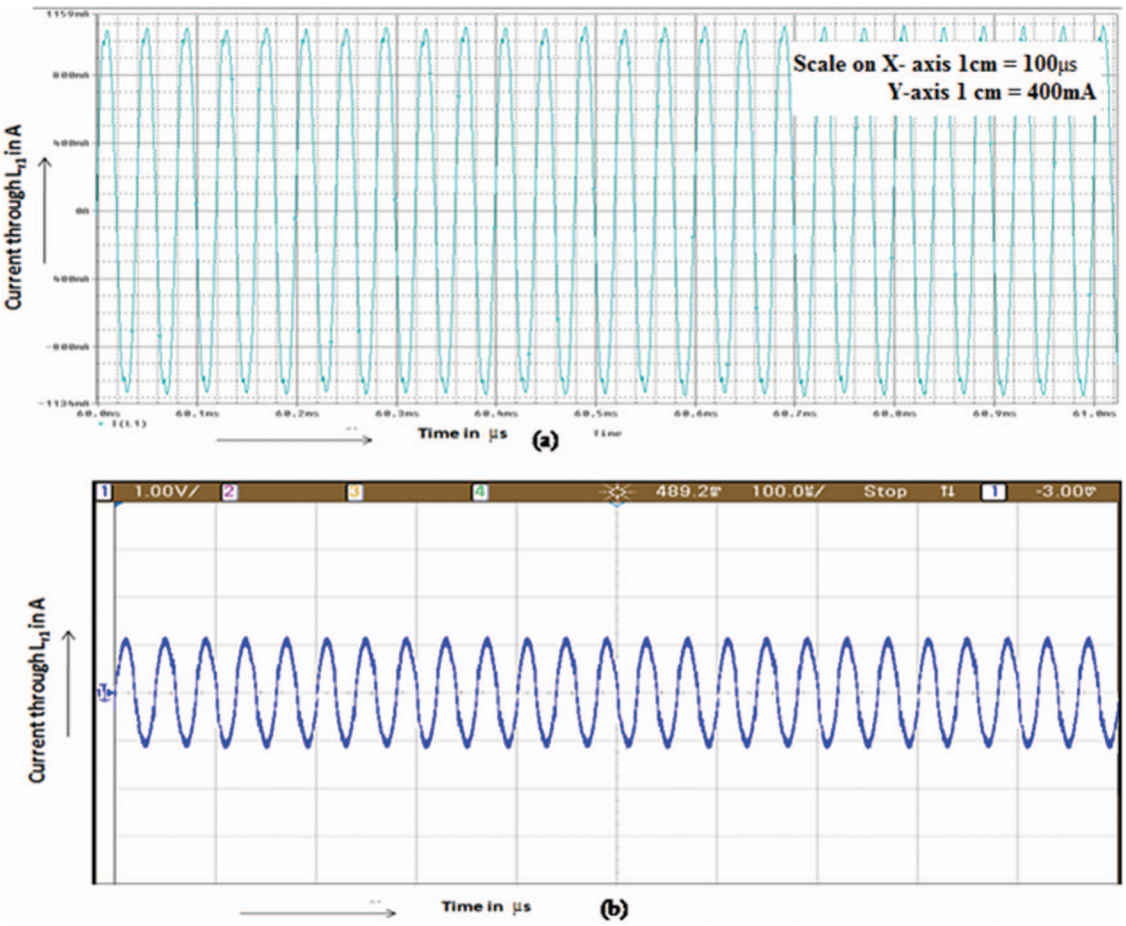

FIG. 10. Magnified waveform of current through resonant inductor L_{r1}. (a) Simulated; (b) experimental.

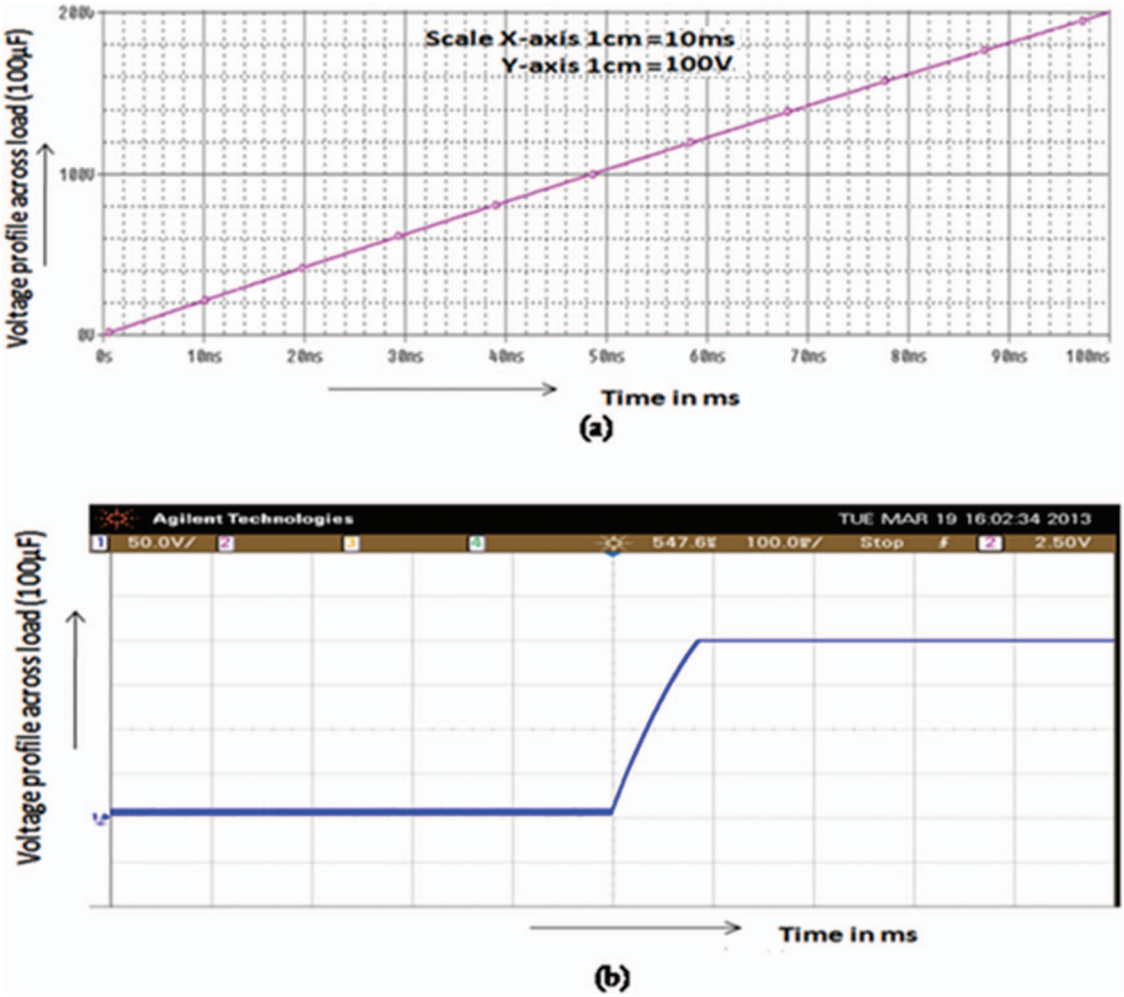

FIG. 11. Voltage profile across load capacitor (100 μF). (a) Simulated; (b) experimental.

Fig. 11(a) and observed that the load capacitor (100 μF) charged to 200 V in 100 ms. Fig. 12(a) describes the zero current switching (ZCS) of inverter switches with respect to inverter output voltage, it is observed that switches M_1 and M_2 turned on and turned off for every 20 μs.

B. Experimental results

The proposed LCLC converter utilized both ZCS and ZVS for smooth switching action, which can improve the overall efficiency of the converter by reducing the losses in the inverter circuit. Experimental results are validated with the simulation results. The prototype setup is shown in Fig. 13. Current profile through resonant inductor L_{r1} is shown in Fig. 9(b) which increases linearly with the progress in time and its magnified wave form is shown in Fig. 10(b). By observing both simulation and experimental results, it is observed that the current flowing through the resonant inductor is almost same as that of simulation results. Fig. 4 which has already been shown in Sec. II, describes the voltage profile across resonant capacitor, which is useful in finding the peak current flowing through the switches M_1 and M_2.

The proposed topology is meant for capacitor charging power supply (CCPS) application, interested in charging profile as shown in Fig. 11(b). It is observed that the load capacitor is charged to 200 V in 100 ms. Experimental results which are shown in Figs. 12(a) and 7 are verified with simulation results to ensure ZCS and ZVS. In Fig. 12(b) it is observed that the current through resonant inductor (L_{r1}) and inverter output are in same phase (i.e., the switching action takes place in inverter switches when the current through the switch is zero). Fig. 7 describes ZVS, it can be explained by comparing pulse width modulation (pwm) pulses for MOSFET switches and current flowing through M_1, M_2, D_1, and D_2 with respect to time. Switching action takes place in inverter switches when the voltage across the switch is zero is shown in Fig. 7. Explanation is as follows, when the switch M_1 is turned off the current will not become zero immediately it tried to flow in same direction, then it chooses the path resonant network—D_2–C_2. In the very next instant of time, when switch M_2 is about to start the voltage across the switch is zero (i.e., the switch M_2 turned on at zero voltage). On the other hand when switch M_2 is turned off the current will not become zero immediately it tried to flow in same direction, then it chooses the path resonant network—D_1–C_1. In the very next instant of time, when

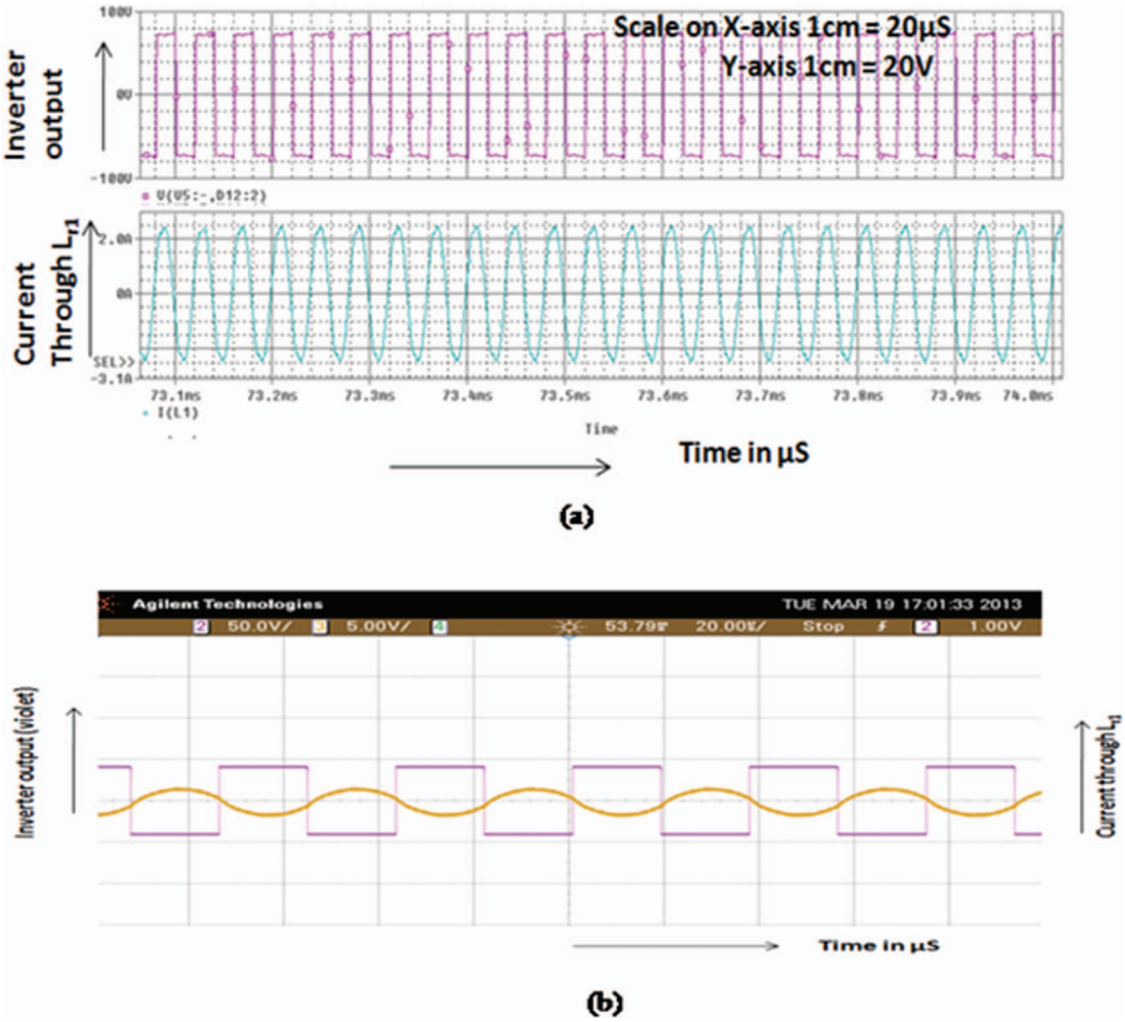

FIG. 12. Magnified current waveform through L_{r1} vs voltage across inverter to ensure ZCS. (a) Simulated; (b) experimental.

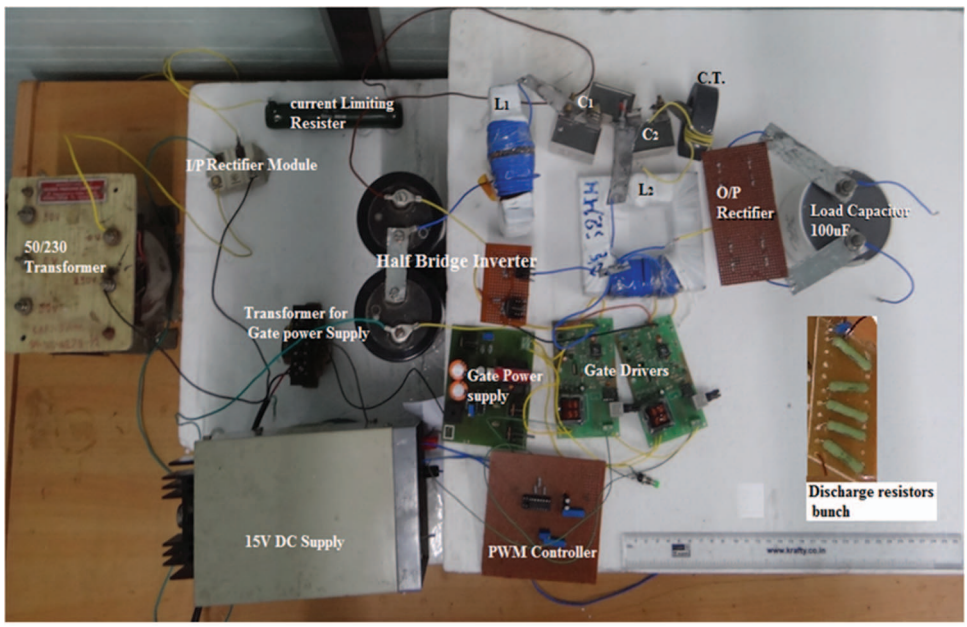

FIG. 13. Prototype set up of fourth order (LCLC) resonant based capacitor charging power supply.

switch M_1 is about to start the voltage across the switch is zero (i.e., the switch M_2 turned on at zero voltage).

V. CONCLUSIONS

Fourth order LCLC resonant converter analyzed and carried out mathematical analysis for finding out load independent current and condition for ZCS. A prototype based 20 J/s capacitor charging power supply designed, developed, and tested successfully by charging 100 μF load capacitor in $\approx$100 ms. The experimental results obtained from prototype are more or less same as simulation results. Proposed design efficiency is $>$90% without high frequency transformer. The design utilized both soft switching techniques such as ZCS and ZVS by adjusting dead time, to improve the converter efficiency and verified the experimental results with simulation results. This paper is confined to introduce a new resonant converter topology with smaller rating (20 J/s) for capacitor charging power supply, the operation verified with prototype and the system works satisfactorily, experimental results matched with simulation results.

The proposed design having limitations such as the number of resonant components increases and in high power systems transformer components may be dominant compared to resonant components. Care must be taken in designing high frequency transformer; these components should not alter the working principle of resonant converter.

ACKNOWLEDGMENTS

We would like to express our sincere thanks to Dr. L. M. Gantayet, Group Director BTD group for constant encouragement and support. We would like to place on record our sincere thanks to Ranjeet, S. G. Patil, and Vaithy for technical help.

[1]H. Akiyama, T. Sakugawa, and T. Namihira, IEEE Trans. Dielectr. Electr. Insul. **14**(5), 1051–1064 (2007).
[2]H. Zhong, Z. Xu, X. Zou, L. Yang, and Z. Chao, in *The 29th Annual Conference of the IEEE Industrial Electronics Society* (IECON 2003), 2–6 November 2003, Vol. 1, pp. 373–377 (2003).
[3]M. Borage, "Parallel resonant converter as a current source," J. Indian Inst. Sci. **83**, 117–125 (2003).
[4]M. Borage, S. Tiwari, and S. Kotaiah, IEEE Trans. Ind. Electron. **54**, 741–746 (2007).
[5]A. Patel, K. V. Nagesh, T. Kolge, and D. P. Chakravathy, Rev. Sci. Instrum. **82**(4), 045111 (2011).
[6]M. B. Borge, "Resonant converter topologies for constant-current power supplies and their applications," Ph.D. thesis (HBNI, 2011).